Thermoelastic Effect on Delta-Wing Flutter with Arbitrary Stiffness Orientation

TSAI-CHEN SOONG*
Xerox Corporation, Rochester, N.Y.

An energy method is derived for vibration and flutter of built-up delta-wings with thermoelastic effect included. The necessary equations for beam-type members and layered anisotropic plates are tabulated so that structures using such members as components can be easily analyzed for static and dynamic problems with arbitrary thermal gradient and stiffness orientations. A large, built-up delta-wing of NACA with assumed temperature distribution was used for analytical studies. Preliminary results showed that with constant ambient temperature, flutter speed is increased when spars, stiffeners, and major stiffness direction of plates are made to be parallel to, or swept back more than, the leading edge of the wing. Flutter characteristics are compared for delta-wings of isotropic skin, stiffened skin, honeycomb sandwich, and corrugated sandwich skin of equal weight with component orientations and stiffness directions of skin varied. For an assumed temperature distribution which is constant along boundaries of the wing and lower in the interior, thermal effect on vibration and flutter seemed to be less significant when stiffners were placed at sweep-back positions than at sweep-forward positions.

Nomenclature

A = cross section area of stiffener
$D_\xi, D_\eta, D_{\xi\eta}$ = bending stiffnesses for orthotropic plates in ξ-η axes
E, G = Young's and shear moduli of isotropic plate
E_{11}, E_{22}, G_{12} = Young's and shear moduli of orthotropic layers in ξ-η plane
g = gravity
$G_r J_r$ = St. Venant's torsional rigidity of stiffeners or beams
I_r, I_{or} = moment of inertia of stiffener with respect to its own neutral axis and to reference plane of wing, respectively
I_{xx}, I_{yy} = moments of inertia of concentrated weight, Eq. (27)
l_r = stiffener spacing measured perpendicular to stiffeners
L = length, Eq. (31)
m,n = $\cos\theta$ and $\sin\theta$, respectively; also integer subscripts
$M, \bar{M}$ = Mach number and Mach number parameter, Eq. (33)
M_x, M_y, M_{xy} = moment resultants in x-y plane, Eq. (9)
N_x, N_y, N_{xy} = stress resultants in x-y plane, Eq. (8)
$\bar{N}_x, \bar{N}_y, \bar{N}_{xy}$ = inplane prestress resultants; tension is positive
$q(x,y)$ = pressure load per unit area
$Q_{ij}, \bar{Q}_{ij}$ = stiffnesses in ξ-η plane and x-y plane, respectively
R_x, R_y = radii of curvature of curved plate
t = time; also thickness of plate, Table 1
T, T_k = temperature and kth layer temperature, respectively
U = velocity of freestream at infinity
u,v,w = deflections at the reference plane of wing
W = weight of concentrated load, Eq. (27)
z = distance referred to local reference plane
z_o = distance from reference plane of plate to reference plane of wing
z_r = distance from neutral axis of stiffener to reference plane of wing
σ, τ = stresses
α_ξ, α_η = thermal coefficients in ξ-η coordinates
$\bar{\sigma}_{r\xi}$ = prestress of beam along ξ-direction, Eq. (33)
Γ_r = warping constant of stiffener or beam
$\bar{\varepsilon}$ = strain at reference plane, Eq. (7)
$\varepsilon_x, \varepsilon_y, \gamma_{xy}$ = strains in coordinate system x-y, Fig. 1
$\varepsilon_\xi, \varepsilon_\eta, \gamma_{\xi\eta}$ = strains in coordinate system ξ-η or 1-2 system
θ = angle of inclination of stiffener, Fig. 1
$\bar{\theta}_1, \bar{\theta}_2, \bar{\theta}_3$ = temperature parameters, Eq. (1)
$\nu, \nu_{12}', \nu_{21}'$ = Poisson's ratios (extensional)
$\nu_\xi', \nu_\eta', \nu_\xi, \nu_\eta$ = extensional and bending Poisson's ratios of plate
ρ_a = mass density of air
ρ_p, ρ_r = weight density of plate and stiffner, lb/volume
$\omega, \bar{\omega}$ = frequency, rad/sec; and frequency parameter, Eq. (33)
$[\,], \{\,\}$ = square, column (or row) matrices

Subscripts

k = numbering of layers, Fig. 1
m,n = integer subscripts, Eq. (31)
r = refer to beam-type stiffener
x,y = coordinates of reference plane of wing
ξ,η = local coordinates (principal axes of orthotropy)

Presented as Paper 72-174 at the AIAA 10th Aerospace Sciences Meeting, San Diego, Calif., January 17–19, 1972; submitted January 27, 1972; revision received September 8, 1972. The author acknowledges the assistance of C. Li of the Boeing Computer Service for numerical computations. The study was completed while the author was a Senior Research Specialist of the Commercial Airplane Group, The Boeing Company, Seattle, Wash.

Index categories: Aircraft Performance, Aircraft Structural Design (Including Loads); Aircraft Vibration.

* Senior Engineering Specialist.

Introduction

AN important structural aspect of stiffened panels and built-up structures is the effect of orientation of components and direction of stiffness anisotropy on such static and dynamic behaviors as vibrations and flutter. Calligeros and Dugundji[1] and Bohon[2] have studied orthotropic panels under arbitrary flow and arbitrary stiffness orientations. Their results indicate appreciable effects on flutter boundary when stiffness orientation is changed for certain aspect ratios of the panel. Turner[3] used a finite-element approach to optimize proportions of structural components to attain a flutter requirement with minimum total mass of an airplane. It was a contribution in optimization with dynamic constraints for structures with prescribed geometry. However, its extension to the subject matter would be impractical since a finite-element analysis requires ab initio a definite structural layout. Each time a component changed its orientation, a new mesh matrix and, correspondingly, a new stiffness matrix would have to be calculated. At present, there does not seem to be an approximate (but general) method or procedure which emphasizes easy manipulations of the stiffness orientation of component members and which could yield quick estimates of their effect on static and dynamic behaviors of a built-up structure. To provide such a capability in analysis is one objective of the present paper.

The second objective is to obtain useful design informations with respect to vibration and flutter characteristics of a typical built-up delta-wing in thermal environment. This is accomplished by studying a linearly tapered, built-up delta-wing

which is described in a NACA report.[4] For constant ambient temperature, the calculated vibration frequencies and mode shapes were correlated with test data. Vibration frequencies and flutter speeds were calculated for different combinations of inclinations of skin-stiffener, rib and spars with the weight distributions remaining unchanged. Four types of skin constructions of equal weight were studied, namely, isotropic skin with parallel skin-stiffeners which possess cross sectional area but no bending rigidity, constant skin, honeycomb sandwich skin, and corrugated sandwich skin. The first type of skin resembled a wing surface stiffened by unidirectional, composite strips or stiffeners with low bending rigidity.

For the case of variable temperature, a temperature distribution which is constant around the circumference and lower in the interior is superimposed on the previous wing as an example. The corresponding thermal stress and its effect on vibration frequencies and flutter for various stiffener angles were studied. Such numerical results can be useful in preliminary studies of supersonic wings when optimal flutter control is an objective.

The present method can be used with existing automated optimization programs as an additional constraint on vibration, flutter and dynamic responses. Such capability of optimally reorienting structural stiffeners, taking account of thermal environment, seems not yet available in current programs.

Derivation of Equations

For generality in applications, assume that the skin of a structure is a layered plate. Each layer is orthotropic but arbitrarily oriented, with a given temperature distribution $T = T(x,y,z)$. Figure 1 shows the sign convention. The stress-strain relationships of the kth layer with respect to x,y axes of the plate are

$$\begin{Bmatrix}\sigma_x\\ \sigma_y\\ \tau_{xy}\end{Bmatrix}_k = \begin{bmatrix}\bar{Q}_{11} & \bar{Q}_{12} & \bar{Q}_{16}\\ \bar{Q}_{12} & \bar{Q}_{22} & \bar{Q}_{26}\\ \bar{Q}_{16} & \bar{Q}_{26} & \bar{Q}_{66}\end{bmatrix}_k \begin{Bmatrix}\varepsilon_x - \varepsilon_x{}^T\cdot T\\ \varepsilon_y - \varepsilon_y{}^T\cdot T\\ \gamma_{xy} - \gamma_{xy}{}^T\cdot T\end{Bmatrix}_k$$
$$= [\bar{Q}_{ij}]_k \begin{Bmatrix}\varepsilon_x\\ \varepsilon_y\\ \gamma_{xy}\end{Bmatrix}_k - \begin{Bmatrix}\bar{\theta}_1\\ \bar{\theta}_2\\ \bar{\theta}_3\end{Bmatrix}_k T \quad (1)$$

The $\bar{Q}_{ij}$ matrix is related to the corresponding matrix of ξ,η axes by a transformation matrix (see Ref. 5 for details). The resulting equations are

$$\begin{aligned}
\bar{Q}_{11} &= Q_{11}m^4 + 2(Q_{12} + Q_{66})m^2n^2 + Q_{22}n^4\\
\bar{Q}_{22} &= Q_{11}n^4 + 2(Q_{12} + Q_{66})n^2m^2 + Q_{22}m^4\\
\bar{Q}_{12} &= (Q_{11} + Q_{22} - 2Q_{66})m^2n^2 + Q_{12}(m^4 + n^4)\\
\bar{Q}_{66} &= 2[(Q_{11} + Q_{22} - 2Q_{12} - Q_{66})m^2n^2 + \tfrac{1}{2}Q_{66}(m^4 + n^4)]\\
\bar{Q}_{16} &= 2[(Q_{11} - Q_{12} - Q_{66})m^2 + (Q_{12} - Q_{22} + Q_{66})n^2]mn\\
\bar{Q}_{26} &= 2[(Q_{11} - Q_{12} - Q_{66})n^2 + (Q_{12} - Q_{22} + Q_{66})m^2]mn
\end{aligned} \quad (2)$$

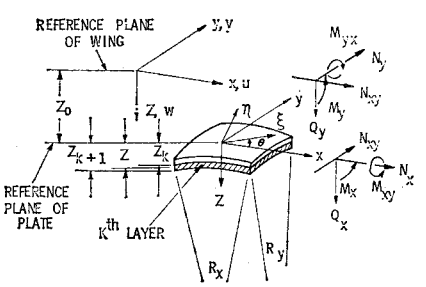

Fig. 1 Coordinate systems and sign conventions of layered plate.

where $m = \cos\theta$, $n = \sin\theta$ and the $[Q_{ij}]$ matrix are:

$$\begin{aligned}
Q_{11} &= E_{11}/(1 - \nu_{21}'\nu_{12}');\ Q_{22} = E_{22}/(1 - \nu_{12}'\nu_{21}')\\
Q_{12} &= Q_{21} = E_{11}\nu_{21}'/(1 - \nu_{12}'\nu_{21}')\\
&= E_{22}\nu_{12}'/(1 - \nu_{12}'\nu_{21}')\\
Q_{66} &= Q_{12}
\end{aligned} \quad (3)$$

Definitions of notations are given in the Nomenclature.

On the thermal part of Eq. (1), one has

$$\varepsilon_x{}^T = m^2\alpha_\xi + n^2\alpha_\eta,\ \varepsilon_y{}^T = n^2\alpha_\xi + m^2\alpha_\eta,\ \varepsilon_{xy}{}^T = mn(\alpha_\xi - \alpha_\eta) \quad (4)$$

and the unit thermal stresses are

$$\begin{aligned}
\bar{\theta}_1 &= (m^2Q_{11} + n^2Q_{12})\alpha_\xi + (m^2Q_{12} + n^2Q_{22})\alpha_\eta\\
\bar{\theta}_2 &= (n^2Q_{11} + m^2Q_{12})\alpha_\xi + (n^2Q_{12} + m^2Q_{22})\alpha_\eta\\
\bar{\theta}_3 &= [(Q_{11} - Q_{12})\alpha_\xi + (Q_{12} - Q_{22})\alpha_\eta]mn
\end{aligned} \quad (5)$$

Based on expressions for the kth layer, written in x-y coordinates, the elastic strain energy of the whole plate is

$$U_p = 1/2\iiint [\sigma_x(\varepsilon_x - \varepsilon_x{}^T T) + \sigma_y(\varepsilon_y - \varepsilon_y{}^T T) + \tau_{xy}(\gamma_{xy} - \gamma_{xy}{}^T T)]dz\,dx\,dy \quad (6)$$

To derive a general expression for the strain energy of a plate in terms of displacements u, v, and w of a distant reference plane, it is convenient to imagine that the plate is the skin of a wing which has curvatures $1/R_x$ and $1/R_y$ at a point (x,y) in the midplane of the wing. z_o is the distance from the reference plane of the plate to the midplane of the wing whose displacements are denoted by u, v, and w as in Fig. 1. The curvatures are assumed to be constant through the thickness of the wing section which is assumed to be small compared with the other two dimensions of the wing. The unit strains at the kth layer can be written as

$$\begin{aligned}
\varepsilon_x &= \bar{\varepsilon}_x - (z_o + z)w_{,xx} = u_{,x} - (w/R_x) - (z_o + z)w_{,xx}\\
\varepsilon_y &= \bar{\varepsilon}_y - (z_o + z)w_{,yy} = v_{,y} - (w/R_y) - (z_o + z)w_{,yy}\\
\gamma_{xy} &= \bar{\gamma}_{xy} - 2(z_o + z)w_{,xy} = u_{,y} + v_{,x} - 2(z_o + z)w_{,xy}
\end{aligned} \quad (7)$$

where the subscript comma denotes partial differentiation with respect to the subscript(s) that follow.

The stress resultants and moments at the reference plane of the plate are given by

$$\begin{Bmatrix}N_x\\ N_y\\ N_{xy}\end{Bmatrix} = [A_{ij}]\begin{Bmatrix}u_{,x} - (w/R_x) - z_ow_{,xx}\\ v_{,y} - (w/R_y) - z_ow_{,yy}\\ u_{,y} + v_{,x} - 2z_ow_{,xy}\end{Bmatrix} - [B_{ij}]\begin{Bmatrix}w_{,xx}\\ w_{,yy}\\ 2w_{,xy}\end{Bmatrix} - \begin{Bmatrix}N_1{}^T\\ N_2{}^T\\ N_3{}^T\end{Bmatrix} \quad (8)$$

$$\begin{Bmatrix}M_x\\ M_y\\ M_{xy}\end{Bmatrix} = [B_{ij}]\begin{Bmatrix}u_{,x} - (w/R_x) - z_ow_{,xx}\\ v_{,y} - (w/R_y) - z_ow_{,yy}\\ u_{,y} + v_{,x} - 2z_ow_{,xy}\end{Bmatrix} - [D_{ij}]\begin{Bmatrix}w_{,xx}\\ w_{,yy}\\ 2w_{,xy}\end{Bmatrix} - \begin{Bmatrix}M_1{}^T\\ M_2{}^T\\ M_3{}^T\end{Bmatrix} \quad (9)$$

where the subscript, ij, of matrices A, B, and D, follows those of the stiffness matrix $\bar{Q}_{ij}$ in Eq. (1). The A, B, D matrices and the thermal stress resultants N^T and moments M^T are given by

$$\{A_{ij},B_{ij},D_{ij}\} = \sum_{k=1}^{N_0}\int_{z_k}^{z_{k+1}} [\bar{Q}_{ij}]_k\{1,z,z^2\}dz \quad (10)$$

$$ij = 11,12,16,22,26,66$$

$$\{N_i{}^T,M_i{}^T\} = \sum_{k=1}^{N_0}\int_{z_k}^{z_{k+1}} (\bar{\theta}_i)_k\{1,z\}T(x,y,z)dz \quad i = 1,2,3 \quad (11)$$

After integration through the thickness of the plate, one obtains from Eq. (6),

$$\begin{aligned}
U_p = 1/2\iint [&(N_x - N_1{}^T)(\bar{\varepsilon}_x - z_ow_{,xx}) +\\
&(N_y - N_2{}^T)(\bar{\varepsilon}_y - z_ow_{,yy}) +\\
&(N_{xy} - N_3{}^T)(\bar{\gamma}_{xy} - 2z_ow_{,xy}) - (M_x - M_1{}^T)w_{,xx} -\\
&(M_y - M_2{}^T)w_{,yy} - 2(M_{xy} - M_3{}^T)w_{,xy}]dxdy
\end{aligned} \quad (12)$$

Table 1 Stiffness constants in strain energy expression of Eqs. (13) and (19)

Symbol	I Layered orthotropic plate	II Isotropic plate	III Inclined beam-type stiffeners
g_1	A_{11}	$Et/(1-\nu^2)$	$E_r A_r \cos^4\theta$
g_2	A_{66}	Gt	$\frac{1}{4}E_r A_r \sin^2 2\theta$
g_3	A_{22}	g_1	$E_r A_r \sin^4\theta$
g_4	A_{12}	νg_1	$\frac{1}{4}E_r A_r \sin^2 2\theta$
g_5	$A_{11}z_o^2 + 2B_{11}z_o + D_{11}$	$g_1 z_o^2 + D$	$\frac{1}{4}G_r J_r \sin^2 2\theta + E_r I_{or} \cos^4\theta$[a]
g_6	$4A_{66}z_o^2 + 8B_{66}z_o + 4D_{66}$	$4Gtz_o^2 + \frac{1}{3}Gt^3$	$G_r J_r \cos^2 2\theta + E_r I_{or} \sin^2 2\theta$
g_7	$A_{22}z_o^2 + 2B_{22}z_o + D_{22}$	$g_1 z_o^2 + D$	$\frac{1}{4}G_r J_r \sin^2 2\theta + E_r I_{or} \sin^4\theta$
g_8	$A_{12}z_o^2 + 2B_{12}z_o + D_{12}$	$\nu(g_1 z_o^2 + D)$	$\frac{1}{4}\sin^2 2\theta(-G_r J_r + E_r I_{or})$
g_9	$A_{11}z_o + B_{11}$	$g_1 z_o$	$E_r A_r z_r \cos^4\theta$
g_{10}	$A_{12}z_o + B_{12}$	$\nu g_1 z_o$	$\frac{1}{4}E_r A_r z_r \sin^2 2\theta$
g_{11}	$A_{66}z_o + B_{66}$	Gtz_o	$\frac{1}{4}E_r A_r z_r \sin^2 2\theta$
g_{12}	$A_{22}z_o + B_{22}$	$g_1 z_o$	$E_r A_r z \sin^4\theta$
g_{13}	A_{16}	0	$\frac{1}{2}\sin 2\theta E_r A_r \cos^2\theta$
g_{14}	A_{26}	0	$\frac{1}{2}\sin 2\theta E_r A_r \sin^2\theta$
g_{15}	$2A_{16}z_o + 2B_{16}$	0	$\sin 2\theta E_r A_r z_r \cos^2\theta$
g_{16}	$2A_{26}z_o + 2B_{26}$	0	$\sin 2\theta E_r A_r z_r \sin^2\theta$
g_{17}	$2A_{16}z_o^2 + 4B_{16}z_o + 2D_{16}$	0	$\frac{1}{2}\sin 2\theta(-G_r J_r \cos 2\theta + 2E_r I_{or} \cos^2\theta)$
g_{18}	$2A_{26}z_o^2 + 4B_{26}z_o + 2D_{26}$	0	$\frac{1}{2}\sin 2\theta)G_r J_r \cos 2\theta + 2E_r I_{or} \sin^2\theta)$

[a] $I_{or} = I_r + A_r z_r^2$.

where a term $f(T)$ has been omitted in the right-hand side of Eq. (12), since it will vanish in the later variational process.

When temperature distribution is prescribed, Eqs. (11) and (12) can be calculated which may include the general case where the material properties are temperature-dependent. Substitution of Eqs. (7–9) into Eq. (12) yields

$$U_p = 1/2 \iint (I(x,y) - 2\{N_1{}^T[u_{,x} - (w/R_x) - z_o w_{,xx}] + N_2{}^T[v_{,y} - (w/R_y) - z_o w_{,yy}] + N_3{}^T(u_{,y} + v_{,x} - 2z_o w_{,xy}) - M_1{}^T w_{,xx} - M_2{}^T w_{,yy} - 2M_3{}^T w_{,xy}\})dxdy \quad (13)$$

The quantity $I(x, y)$ is given by

$$I(x,y) = g_1(u_{,x} - w/R_x)^2 + g_2(u_{,y} + v_{,x})^2 + g_3(v_{,y} - w/R_y)^2 + 2g_4(u_{,x} - w/R_x)(v_{,y} - w/R_y) + g_5 w_{,xx}{}^2 + g_6 w_{,xy}{}^2 + g_7 w_{,yy}{}^2 + 2g_8 w_{,xx}w_{,yy} - 2[(u_{,x} - w/R_x)\cdot(g_9 w_{,xx} + g_{10}w_{,yy}) + 2g_{11}w_{,xy}(u_{,y} + v_{,x}) + (v_{,y} - w/R_y)(g_{10}w_{,xx} + g_{12}w_{,yy})] + 2\{(u_{,y} + v_{,x})\cdot[g_{13}(u_{,x} - w/R_x) + g_{14}(v_{,y} - w/R_y) - 1/2(g_{15}w_{,xx} + g_{16}w_{,yy})] + w_{,xy}[g_{17}w_{,xx} + g_{18}w_{,yy} - g_{15}(u_{,x} - w/R_x) - g_{16}(v_{,y} - w/R_y)]\} \quad (14)$$

where g_1 to g_{18} are given in column 1 of Table 1. In Table 1, column 1 is applicable to general layered plates in which each layer is homogeneous, orthotropic with arbitrary material properties and thickness, and arbitrarily inclined. Column II is a special case of column I for an isotropic plate with thickness t. Column III is for beam-type structural components which will be derived later.

The constants in Column I of Table 1 for some special cases, such as homogeneous orthotropic plate, honeycomb sandwich plate and corrugated plate, are given in Ref. 5 for reference.

Equations for Beam-Type Structural Components

Beam-type structural components may include spars and ribs of wings, stringers and ring frames of fuselages and integral stiffeners in skin plates. Assuming that ξ is the axis of a beam which makes an angle θ with the x-axis of the plate, as shown in Fig. 1, the elastic strain energy of the beam due to Kirchhoff-Love type displacements at the reference plane of the wing section can be written as

$$U_r = \frac{1}{2}\int\left[\int_{A_r} E_r\varepsilon_{\xi r}{}^2 dA_r + G_r J_r(w_{,\xi\eta})^2 + E_r\Gamma_r(w_{,\xi\xi\eta})^2\right]d\xi \quad (15)$$

where the first term in the integrand corresponds to axial strain $\varepsilon_{\xi r}$ of an elementary area dA_r of the cross section of the beam, the second term is due to Saint Venant torsion and the third term is from warping considerations. The warping constant Γ_r of different beam sections can be found, for example, in Ref. 6.

The coordinate relations between the two sets of orthogonal systems are

$$x = \xi\cos\theta - \eta\sin\theta; \quad y = \xi\sin\theta + \eta\cos\theta \quad (16)$$

The strain in the ξ direction of an element, at an eccentric distance $(z_r + z)$ from the reference plane whose displacements are u, v, and w, is

$$\varepsilon_{\xi r} = \bar{\varepsilon}_\xi - (z_r + z)w_{,\xi\xi} - \alpha_r T \quad (17)$$

converted into x, y coordinates, Eq. (17) becomes

$$\varepsilon_{\xi r} = \bar{\varepsilon}_x\cos^2\theta + \tfrac{1}{2}\bar{\gamma}_{xy}\sin 2\theta + \bar{\varepsilon}_y\sin^2\theta - (z_r + z)(w_{,xx}\cos^2\theta + w_{,xy}\sin 2\theta + w_{,yy}\sin^2\theta) - \alpha_r T \quad (18)$$

After substitution of $\varepsilon_{\xi r}$ and $w_{,\xi\eta}$, $w_{,\xi\xi\eta}$, which can be obtained with the aid of Eq. (16), into Eq. (15) and integration over the cross section of the beam, one obtains the elastic strain energy of a discrete, inclined beam whose neutral axis has an eccentric distance z_r with respect to a reference plane, say the mid-plane of a wing section: (terms contain T^2 are dropped)

$$U_r = \frac{1}{2}\int\Bigg\{I(x,y) - 2\Bigg[\left(u_{,x} - \frac{w}{R_x}\right)\cos^2\theta + \frac{1}{2}(u_{,y} + v_{,x})\sin 2\theta + \left(v_{,y} - \frac{w}{R_y}\right)\sin^2\theta\Bigg]N_r{}^T + 2[w_{,xx}\cos^2\theta + w_{,xy}\sin 2\theta + w_{,yy}\sin^2\theta]M_r{}^T + E_r\Gamma_r\Bigg[-\frac{1}{2}w_{,xxx}\sin 2\theta\cos\theta + w_{,xxy}\left(\cos 2\theta\cos\theta - \frac{1}{2}\sin 2\theta\sin\theta\right) + w_{,xyy}\left(\frac{1}{2}\sin 2\theta\cos\theta + \cos 2\theta\sin\theta\right) + \frac{1}{2}w_{,yyy}\sin 2\theta\sin\theta\Bigg]^2\Bigg\}d\xi \quad (19)$$

The expression $I(x,y)$ is the same as expressed by Eq. (14) and the corresponding values of g_1 to g_{18} for beam-type components are given in column III of Table 1. The thermal terms in Eq. (19) are given by

$$\{N_r^T, M_r^T\} = \int_{A_r} E_r \alpha_r T\{1, z_r + z\} dA_r \tag{20}$$

If the beams are closely spaced, such as the conventional stiffeners in skin panels, so that their strain energies can be taken as being averaged over the spacing in a given region, Eq. (19) can be written as

$$U_r = \iint \frac{1}{2l_r} (Ix,y) - 2[\cdot\cdot]N_r^T + 2[\cdot\cdot]M_r^T + E_r\Gamma_r[\cdot\cdot]^2) dxdy \tag{21}$$

where l_r is the perpendicular distance between the parallel adjacent beams.

Since $I(x,y)$ of Eq. (14) is used in both Eqs. (13) and (19), the corresponding quantities in the same row of Table 1 can be added to form stiffened plates.

Load Potential Expressions

In the preceding sections, the necessary strain energy expressions for basic building blocks, i.e., beams and plates, for three-dimensional built-up structures have been derived. To complete the total potential, the potential expressions needed in static and dynamic analyses are given in the following:

A. Potential of Lateral Pressure and Prestresses

$$V_1 = -\tfrac{1}{2} \iint [2q(x,y)w - \bar{N}_x(x,y)w_{,x}^2 - \bar{N}_y(x,y)w_{,y}^2 - 2\bar{N}_{xy}(x,y)w_{,x}w_{,y}] dxdy \tag{22}$$

B. Potential of Vibrating Uniform Mass, with Frequency ω

$$\begin{aligned} V_2 &= \tfrac{1}{2} \iiint (\rho_p/g)(\dot{w}^2 + [\dot{u} - (z_o + z)\dot{w}_{,x}]^2 + [\dot{v} - (z_o + z)\dot{w}_{,y}]^2) dxdydz \\ &= -\tfrac{1}{2}\omega^2 \iiint (\rho_p/g)\{w^2 + (u - z_o w_{,x})^2 + (v - z_o w_{,y})^2 + 2z[(u - z_o w_{,x})w_{,x} + (v - z_o w_{,y})w_{,y}] + z^2(w_{,x}^2 + w_{,y}^2)\} dxdydz \end{aligned} \tag{23}$$

where the superscript dot denotes partial derivative with respect to time. For isotropic thin plate with thickness $t(x,y)$, Eq. (23) can be simplified to

$$V_2 = -\frac{\omega^2}{2g} \rho_p \iint \left([w^2 + (u - z_o w_{,x})^2 + (v - z_o w_{,y})^2]t + (w_{,x}^2 + w_{,y}^2)\frac{t^3}{12} \right) dxdy \tag{24}$$

C. Potential of an Inclined Beam Attached to a Vibrating Plate with Frequency ω

The potential is limited here to considerations of inertias along ξ and z only. In terms of u, v, and w of the reference plane, the potential of such an isotropic beam with the rotary moment of inertia included, is

$$\begin{aligned} V_3 = \tfrac{1}{2}(\rho_r/g) \iint_{A_r} &\{\dot{w}^2 + [\dot{u}\cos\theta + \dot{v}\sin\theta - (z_r + z)\cdot (\dot{w}_{,x}\cos\theta + \dot{w}_{,y}\sin\theta)]^2\} dA_r d\xi = -\tfrac{1}{2}\omega^2(\rho_r/g)\cdot \\ &\int (\{w^2 + [(u - z_r w_{,x})\cos\theta + (v - z_r w_{,y})\sin\theta]^2\} A_r + (w_{,x}\cos\theta + w_{,y}\sin\theta)^2 I_r) d\xi \end{aligned} \tag{25}$$

For closely spaced parallel-stiffener systems, Eq. (25) becomes

$$V_3 = -\tfrac{1}{2}\omega^2(\rho_r/l_r g) \iint (\{w^2 + [\cdot\cdot]^2\} A_r + (\cdot\cdot)^2 I_r) dxdy \tag{26}$$

D. Potential of Concentrated Weights

The potential of concentrated weights, with typical weight W and mass moments of inertia I_{xx} and I_{yy} with respect to the x^- and y^- axis, respectively, can be written as

$$V_4 = -\tfrac{1}{2}\omega^2 \sum ((W/g)[w^2 + (u - z_o w_{,x})^2 + (v - z_o w_{,y})^2] + I_{xx}w_{,x}^2 + I_{yy}w_{,y}^2) \tag{27}$$

E. Potential of Aerodynamic Loads Given in Variational Form

For approximate flutter analysis, the variation of the potential of the lateral loading due to aerodynamic pressure based on static strip theory (Ackeret value) is

$$\delta V_5 = \iint \rho_a U^2 (M^2 - 1)^{-1/2}(-w_{,y})\delta w\, dxdy \tag{28}$$

where the negative sign before $w_{,y}$ is added because the y-axis of the wing is opposite to the direction of the freestream. For the "quasi-steady-state" theory, Eq. (28) is replaced by

$$\delta V_5 = \iint \rho_a U^2 (M^2 - 1)^{-1/2}[-w_{,y} + (M^2 - 2)(M^2 - 1)^{-1}(\dot{w}/U)]\delta w\, dxdy \tag{29}$$

Equations (28) and (29) are applicable to small perturbation supersonic flow with $M \geq 1.6$. Structural and aeroviscous dampings are omitted.

F. Total Potential

The total potential of the structure which in general consists of layered skin plate, isotropic skin plate, discrete beams, smeared parallel-beam systems and dead weights, is then the strain energies of these components plus the potential of pre-stresses, vibrating masses and aerodynamic loads. One may write, as a typical expression

$$\Omega = U_p + U_r + V_1 + V_2 + V_3 + V_4 + V_5 \tag{30}$$

Integrating along the area or length of the structural components and adding all the components together, one obtains the total potential of the structure in terms of the reference plane displacements u, v, and w.

Power Series Representation of Displacements

In platelike structures of arbitrary plane form and boundary conditions, a general form for the assumed displacement pattern is a power series. Geometric boundary conditions, such as displacements and slopes, should be enforced and satisfied exactly, whereas natural boundary conditions, such as edge forces and moments, can be left unsatisfied for approximate variational methods.

The analysis will be applied to a built-up delta-wing of NACA.[4] Figure 2 shows the geometry and the coordinates of the specimen. Structural details and a table of component weight distribution in percentages can be found from Refs. 4 and 5, respectively.

Since the given specimen is symmetric with respect to its midplane, an approximate solution can be derived by neglecting the u and v displacements and consider only w. Thus, one may stipulate a displacement at the midplane of the wing

$$w/L = \varphi(x,y) \sum_m \sum_n a_{mn} e^{i\omega t}(x/L)^m (y/L)^n \tag{31}$$

where L is a length used to nondimensionalize x and y, and $\varphi(x,y)$ is a definite function introduced to satisfy the geometric

boundary conditions with respect to w and its derivatives along the boundary. They should vanish when the edges are held against translation and rotation. However, for the present free-free case, $\varphi(x,y)$ is to assume a value of unity.

To facilitate discussions, let the structural components of the half-wing consist of a plate, a discrete beam, a smeared beam and a dead weight of W_1 pound at $x = x_1$ and $y = y_1$. The quasi-steady-state aerodynamic load will be used. It is to be noted that more accurate aerodynamic load expressions could have been used. However, for a preliminary study in which the objective is an indication of a trend rather than quantitative results, the simplicity of the quasi-steady theory may have outweighted its deficiency in relative accuracy.

Assuming that the pre-stresses in Eq. (22) are caused by thermal gradient, then the thermal terms in U_r will be dropped. From Eqs. (13, 19, 21–24, 27, and 29), differentiation of Eq. (30) with respect to an arbitrary amplitude $a_{m'n'}$, leads to the following general equation:

$$\frac{\partial(\Omega/E)}{\partial a_{m'n'}} \sum_m \sum_n a_{mn}[G_1 + (i\bar{\omega})G_2 + (i\bar{\omega})^2 G_3] = 0 \qquad (32)$$

where a common factor $\exp(i\omega t)$ is dropped. The coefficient of a_{mn} is given in the following

$$\bar{\omega} = \omega E^{-1/2} \text{ (frequency parameter)}$$

$$\bar{M} = \rho_a U^2 [E(M^2-1)^{1/2}]^{-1} \text{ (Mach number parameter)}$$

$$G_1 = \left(\iint \left[\sum_{i=1}^{5} \left(\frac{H_i}{E}\right)\left(\frac{x}{L}\right)^{m+m'-i+1}\left(\frac{y}{L}\right)^{n+n'-i+5} + \left(\frac{\bar{N}_x}{E}\right)\left(\frac{x}{L}\right)^{m+m'-2}\left(\frac{y}{L}\right)^{n+n'} mm' + \left(\frac{\bar{N}_y}{E}\right)\left(\frac{x}{L}\right)^{m+m'}\left(\frac{y}{L}\right)^{n+n'-2} nn' + \left(\frac{\bar{N}_{xy}}{E}\right)\left(\frac{x}{L}\right)^{m+m'-1}\left(\frac{y}{L}\right)^{n+n'-1}(mn' + nm')\right]\frac{dxdy}{L^2}\right)_{\text{plate}} +$$

$$\left((1/l_r)\iint \left[\sum_{i=1}^{5}\left(\frac{H_i}{E}\right)\left(\frac{x}{L}\right)^{m+m'-i+1}\left(\frac{y}{L}\right)^{n+n'+i-5} + A_r\left(\frac{\bar{\sigma}_{r\xi}}{E}\right)\left\{\left(\frac{x}{L}\right)^{m+m'-2}\left(\frac{y}{L}\right)^{n+n'} mm'\cos^2\theta + \left(\frac{x}{L}\right)^{m+m'}\left(\frac{y}{L}\right)^{n+n'-2} nn'\sin^2\theta + \left(\frac{x}{L}\right)^{m+m'-1}\left(\frac{y}{L}\right)^{n+n'-1}(mn' + nm')\sin\theta\cos\theta\right\}\right]\frac{dxdy}{L^2}\right)_{\text{smeared beam}} +$$

$$\left(\left(\frac{1}{L}\right)\int[\cdots]\left(\frac{d\xi}{L}\right)_{\text{discrete beam}} - \bar{M}nL^3\iint\left(\frac{x}{L}\right)^{m+m'}\left(\frac{y}{L}\right)^{n+n'-1}\frac{dxdy}{L^2}\right)$$

$$G_2 = \rho_a U[E(M^2-1)]^{-1/2}(M^2-2)(M^2-1)^{-1}L^4 \cdot \iint\left(\frac{x}{L}\right)^{m+m'}\left(\frac{y}{L}\right)^{n+n'}\frac{dxdy}{L^2}$$

$$G_3 = \left(\left(\frac{\rho_p}{g}\right)L^4\iint\left[\left(\frac{x}{L}\right)^{m+m'}\left(\frac{y}{L}\right)^{n+n'}\right]t\frac{dxdy}{L^2}\right)_{\text{plate}} + \left(\left(\frac{\rho_r}{g}\right)\frac{L^4}{l_r}\iint[\cdots]A_r\frac{dxdy}{L^2}\right)_{\text{smeared beam}} + \left(\left(\frac{\rho_r}{g}\right)L^3\int[\cdots]A_r\frac{d\xi}{L}\right)_{\text{discrete beam}} + \left(\left(\frac{w_1}{g}\right)L^2\left(\frac{x_1}{L}\right)^{m+m'}\left(\frac{y_1}{L}\right)^{n+n'}\right)_{\text{dead weight}} \qquad (33)$$

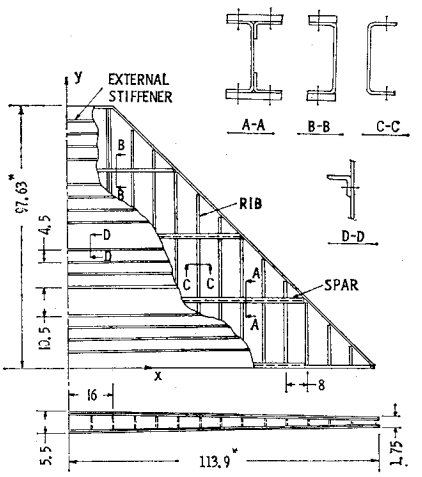

Fig. 2 Geometry of a 45° built-up delta-wing specimen (NACA TN 3999) (Symmetric to centerline, right half shown) Unit: inch. *Dimension of the skin plate. For internal structure dimensions, they are 96 and 112 in., respectively.

where the notation H_i, i from 1 to 5, in G_1 is defined by

$$H_1 = g_7 n(n-1)n'(n'-1)$$

$$H_2 = -g_{18}[mnn'(n'-1) + n(n-1)m'n']$$

$$H_3 = g_8[m(m-1)n'(n'-1) + n(n-1)m'(m'-1)] + g_6 mnm'n'$$

$$H_4 = -g_{17}[mnm'(m'-1) + m(m-1)m'n']$$

$$H_5 = g_5 m(m-1)m'(m'-1) \qquad (34)$$

Equations (32) are linear and homogeneous and the determinant formed by the coefficients of a_{mn} constitutes a complex eigenvalue problem. If G_2 in Eq. (32) is omitted, corresponding to the use of the simple strip theory of Eq. (28), eigenvalues $\bar{\omega}$ shall be real. If, in addition, the flutter parameter $\bar{M}$ in G_1 of Eqs. (33) is omitted, $\bar{\omega}$ in Eqs. (32) is the frequency parameter of the natural vibration.

In Eqs. (32), for the free-free case, $n = 0,1,2\ldots$ and $m = 0,2,4\ldots$ for symmetric modes, $m = 1,3,5\ldots$ for antisymmetric modes. All numerical calculations were made on a CDC 6600 digital computer, with the material constants assumed as $E = 10.6 \times 10^6$psi, $\nu = 0.33$ and $\alpha_\xi = \alpha_\eta = 1.233 \times 10^{-5}$ in./in./°F.

Numerical Results for Vibration and Flutter with Constant Ambient Temperature

The following results were obtained for the case of constant ambient temperature.

A. Effect of Rotatory Inertia and Discreteness; Correlations of Vibration Frequencies and Nodal Line Patterns

Using the 12-term pattern, $n = 0,1,2$, and $m = 0,2,4,6$ or $1,3,5,7$, $L = 100$, the first ten frequencies of free-free vibration excluding the rigid body motions are shown in Table 2. It can be seen that the difference between the most exact formulation as given in "A" and the least exact formulation as given in "D" is rather small for the given specimen. Consequently, in subsequent numerical studies, stiffener and rib systems were smeared and rotatory inertia ignored.

The correlation with experiment shown in Table 2 is not

Table 2 Effect of rotary inertia and discreteness of structural members on vibration frequencies

Mode	Frequency, cps				
	Test	Type of analysis[a]			
	(Ref. 4)	A	B	C	D
1st symmetric	43.4	48.05	47.99	48.14	47.77
1st antisymmetric	52.2				58.58
2nd symmetric	88.8	109.48	108.80	110.09	108.28
2nd antisymmetric	91.7				106.09
3rd symmetric	122.8	162.79	161.87	163.82	161.02
3rd antisymmetric	131.1				168.24
4th symmetric	164.2	213.24	212.89	215.99	212.02
4th antisymmetric	169.2				243.89
5th symmetric	179.9	285.22	284.15	288.37	282.06
5th antisymmetric	215.7				316.69

[a] A—stiffeners, ribs and spars all discrete; rotatory inertia included; B—stiffeners averaged, ribs and spars discrete; rotatory inertia included; C—stiffeners, ribs and spars all discrete; rotatory inertia ignored; D—stiffeners and ribs averaged, spars discrete; rotatory inertia ignored.

very good. However, it should be improved by a more suitable choice of w terms or by use of more terms. The corresponding calculated nodal patterns (type D), on the other hand, agree closely with the test patterns (Fig. 3). It is to be noted that with more restricted but specialized method, better correlation had been obtained for this problem by Kruszewski et al.,[8] who used Levy's influence-coefficient approach[9] that has been corrected for the effect of transverse shear.

B. Effect of Orientation of Skin Stiffeners and Ribs upon Vibration

In orientations studies, it is assumed that structures in the carry-over section remain discrete and fixed; in the triangular parts, the stiffeners and ribs are smeared on their spacings

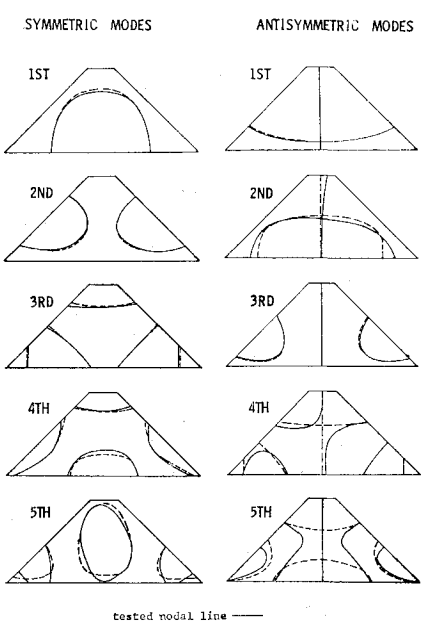

Fig. 3 Correlation of nodal line patterns of free-free vibration modes of the built-up 45° delta-wing specimen (NACA TN 3999).

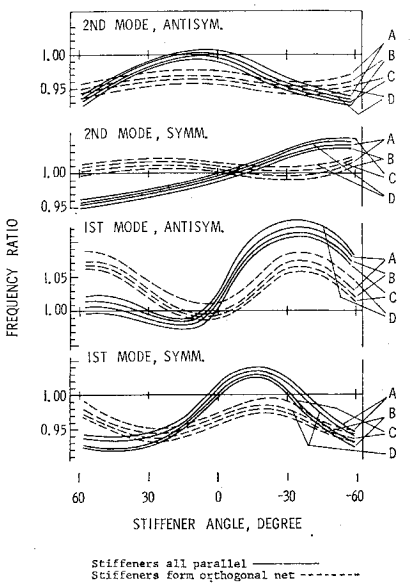

Fig. 4 Frequency ratio vs stiffener angle for four rib angles, 45° wing. Rib angle: A = 0°, B = 45°, C = 90°, D = −45°. Frequencies are compared with specimen with rib angle 90°, stiffener angle 0°, stiffeners all parallel.

and arbitrarily inclined. Spars remain discrete and fixed for the vibration analysis.

If the structural weight per unit length of a beam component is linear with respect to coordinates within a small spacing, which is usually true, then the weight per unit area will remain unchanged when the inclination of the beam is changed provided that the spacing between parallel beams remains the same. This principle will facilitate the study of the effect of orientation of beam-type members for which change of inclination does not bring change in weight distribution of the structure.

In Fig. 4, the ordinate is the frequency ratio, where the calculated frequencies given in Column D of Table 3 are the denominators. Two types of skin-stiffener arrangements were studied; the solid lines are for stiffeners all parallel with a spacing of 6.09 in., which makes the smeared stiffeners equal in length to the discrete system; the dashed lines are for an orthogonal stiffener system with a uniform spacing of 12.18 in. so that the weight of stiffeners remain unchanged. The results indicated that stiffener's effect on vibration frequency is more pronounced than ribs and spars on an equal weight basis. This is probably due to their eccentricity. Furthermore, the parallel arrangement seems to influence the frequency change more than the orthogonal arrangement. The results for modes higher than the second are omitted.

C. Effect of Orientation of Structural Components upon Flutter

In flutter analysis, the structure of the carry-over section remains discrete, but in the triangular parts different types of skin construction were assumed and studied. The basic one is a stiffened skin whose parallel stiffener system has the the same cross-sectional area of the angle-type sitffeners of the NACA specimen, but their eccentricity, bending and torsional stiffnesses about their own neutral axis were omitted. Such construction resembles a skin reinforced by composite strips, or stiffeners with low bending and torsional rigidities. This is the type D skin shown in Fig. 5. The other three, of the same weight per unit area as D, are isotropic constant thickness skin, honeycomb sandwich skin with constant face plates, and 60° corrugated sandwich skin with constant face plates (Fig. 5: A, B, and E, respectively).

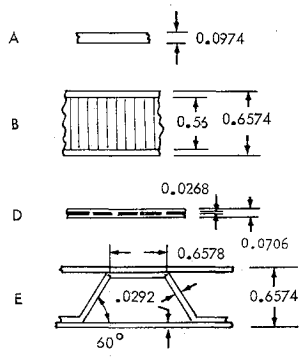

Fig. 5 Geometry of the skins studied. Unit: inch. (All have equal weight per unit area). A—isotropic constant skin; B—honeycomb sandwich skin plate; D—isotropic constant skin with strip type stiffeners that possess cross-sectional area but no bending or torsional rigidities about their own neutral axis; E—60° corrugated sandwich skin.

Some details of the flutter analysis are given in Ref. 5. The final results are given in Fig. 6 which shows that the effect of changing spar angle is much less than that of changing the stiffeners' angle. However, due to the weak orthotrophy of such strip-type stiffeners, the optimum flutter values of curves D are much lower than those corresponding to curves A, B, and E. It seems that if the skin is orthotropic, such as E and D, its orthotropy must be strong in order to surpass the corresponding isotropic types of equal weight and comparable stiffness such as B and A. It probably explains why for symmetric modes the corrugated sandwich type E is superior to the honeycomb sandwich type B, while strip type D is inferior to the corresponding isotropic type A.

Thermal Stress and Its Effect on Vibration and Flutter

As an example of the effect of thermal stress, assume that all the leading and trailing edges of the wing are maintained at a temperature T_1. The center section has a parabolic

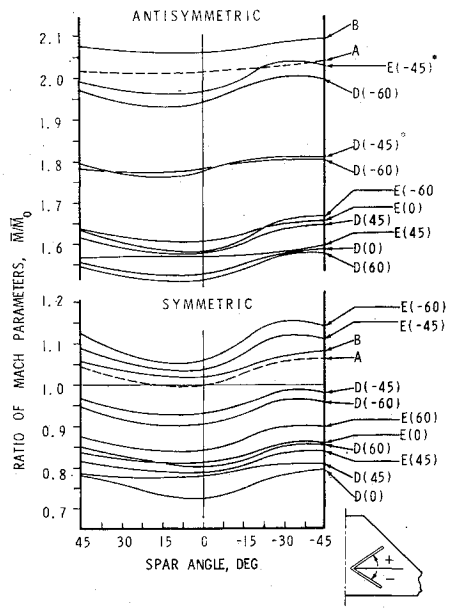

Fig. 6 Ratios of Mach parameters for different spar and stiffness inclinations for the skins of Fig. 5. (Ribs assumed to be perpendicular to spars). *Angle of inclination of stiffeners or corrugations.

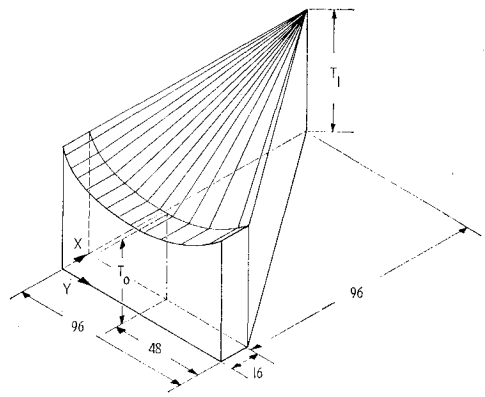

Fig. 7 Schematic diagram for the assumed temperature distribution.

temperature distribution along the y-axis with the lowest temperature T_o located at the midchord. The triangular part has a linear temperature variation towards the tip as shown schematically in Fig. 7. Thus, the equations for the temperature distribution are

$$T(y)|_{0\le x\le 16} = T_1 + (y/24)(T_o - T_1)[1 - (y/96)]$$
$$T(x,y)|_{16\le x\le 112} = T_1 + (y/24)(T_o - T_1)[1 - y/(112 - x)] \tag{35}$$

Such a temperature distribution, if T_1 is put at 450°F and T_o somewhat lower, is not far from the thermal environment of an SST wing cruising at $M = 2.7$ at an altitude of 60,000–70,000 ft.

Since there is no lateral displacement, the thermal displacements in x-y plane can be assumed as

$$u/L = \sum_m \sum_n b_{mn}(x/L)^m(y/L)^n \quad m = 1,3,5,\ldots;\ n = 0,1,2,3\ldots$$
$$v/L = \sum_i \sum_j c_{ij}(x/L)^i(y/L)^j \quad i = 0,2,4,\ldots;\ j = 0,1,2,3,\ldots \tag{36}$$

with the understanding that $c_{00} = 0$ which implies that the origin (0,0) has no displacement. Equations (36) satisfy the requirement that u is antisymmetric and v is symmetric with respect to the y axis.

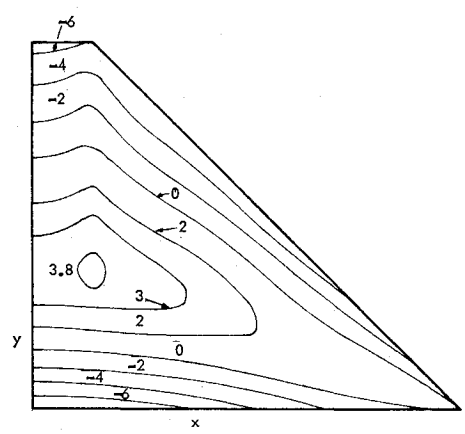

Fig. 8 Contour diagram of thermal strain in x direction, ε_x. Unit: 10^{-4} in./in.. $T_1 = 450°F$, $T_0 = 300°F$, $\nu = 0.33$.

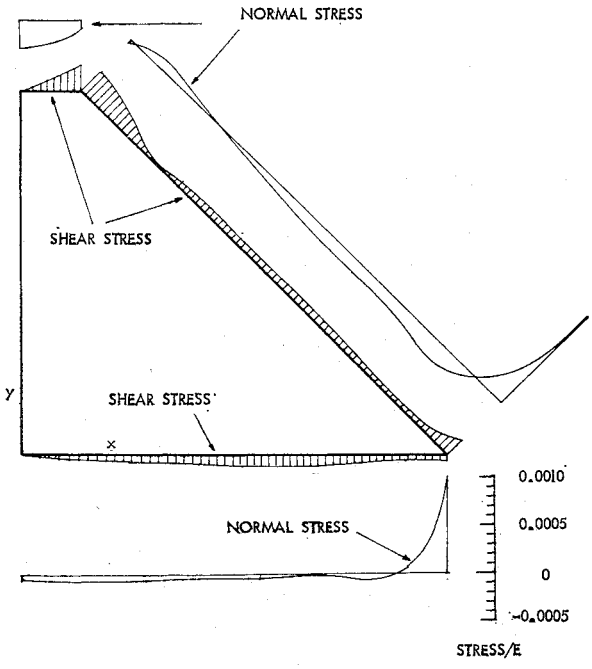

Fig. 9 Thermal stresses at the free edges of the wing plate; $T_1 = 450°F$, $T_0 = 300°F$, $\nu = 0.33$.

Numerical calculations for thermal stress are based on 31-term u and 30-term v (See Ref. 5 for some details), and $L = 112$. Figure 8 is the contour diagram of thermal strain in x direction for an assumed $T_1 = 450°$ and $T_0 = 300°$, thermal strain in y direction and shear strain are given in Ref. 5.

Figure 9 is the calculated normal and shear stresses around the free edges of the wing. These residual quantities seem to be relatively small except near the tips. Figures 10 and 11 show, respectively, the effects on vibration frquencies and flutters due to the presence of such initial thermal stresses for the same wing with its spars and ribs at 0° and 90°, respectively, while the stiffeners in the triangular parts of the wing inclined at various positions.

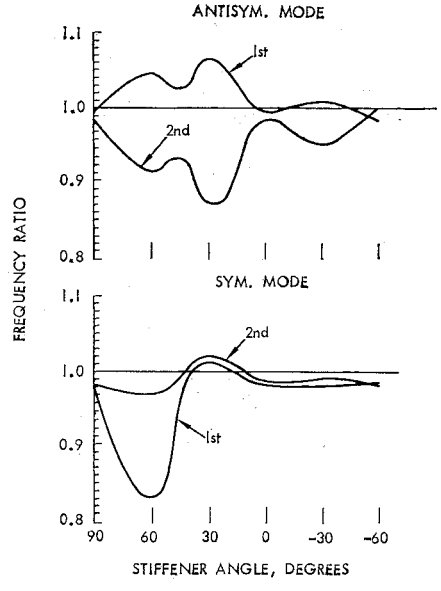

Fig. 10 Ratio of vibration frequencies (frequency with thermal stress divided by frequency without thermal stress) with the same geometry. Stiffener angle changed while spars and ribs remain at 0° and 90°, respectively.

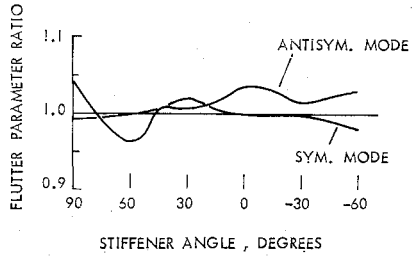

Fig. 11 Ratio of flutter parameters (flutter with thermal stress divided by flutter without thermal stress) with the same geometry. Stiffener angle changed while spars and ribs remain at 0° and 90°, respectively.

Conclusion

Based on the preliminary numerical results from the assumed geometry, one observes that in the case of constant ambient temperature:

1) For delta-wings with stiffened skin, the orientation of stiffeners has considerable effect on its vibration frequencies and supersonic flutter speeds. Inclinations of spar and rib systems seem to have less influence. Compared with a basic configuration in which stiffeners and spars are perpendicular to the centerline of the wing and ribs are parallel to it (0°, 0° and 90°), flutter characteristic can be improved by aligning these beamtype members parallel to, or sweptback more than, the leading edge of the wing. The same observation is true for the optimum stiffness orientation of the corrugated sandwich skin type.

2) For the same unit skin weight, flutter speed decreases according to the following order: corrugated sandwich, honeycomb sandwich, isotropic skin and lastly strip type stiffeners on isotropic skin.

In the case of thermal environment, one observes that the thermal stress distribution obtained by the present method seemed reasonable. However, in the absence of test/analysis correlations, its accuracy cannot be judged. Assuming that it is accurate enough to be taken as initial stresses, then for the given temperature profile, vibration frequencies and flutters seem to be less influenced by the presence of such thermal stresses when stiffeners are inclined backward than when inclined forward. If the assumed temperature profile is reasonably realistic and if the analytic results do not change drastically when details are varied moderately, then by arranging its structural components such that the major stiffness direction is in a sweepback position, a supersonic wing could gain considerably in its flutter performance not only in the increment of flutter speed, but also in its relative insensitivity to thermal cycling.

In conclusion, one observes that besides the usual practice of maneuvering the distribution of weights in a wing to adjust its flutter boundary, the maneuver of stiffness, through changing orientations of structural members and anisotropy of skins, offers another avense for achieving the purpose. It adds a new dimension in an optimal sense for flutter control in constant or variable thermal environment. By maneuvering both weight distribution and stiffness orientation, an optimum configuration of minimum weight for given vibration and flutter constraints can be achieved.

References

[1] Calligeros, J. M., and Dugundji, J., "Effects of Orthotropicity Orientation on Supersonic Panel Flutter," *AIAA Journal*, Vol. 1, No. 9, Sept. 1963, pp. 2180–2182.

[2] Bohon, H. L., "Flutter of Flat Rectangular Orthotropic Panels with Biaxial Loading and Aribtrary Flow Direction," TN D-1949, Sept. 1963, NASA.

[3] Turner, M. J., "Optimization of Structures to Satisfy Flutter Requirements," *AIAA Journal*, Vol. 7, No. 5, May 1969, pp. 945–951.

[4] Kordes, E. E., Kruszewski, E. T., and Weidman, D. J., "Experimental Influence Coefficients and Vibration Modes of a Built-Up 45° Delta-Wing Specimen," TN 3999, May 1957, NACA.

[5] Soong, T. C., "Thermoelastic Effect on Vibration and Flutter of Built-Up Delta-Wings with Arbitrarily Oriented Structural Components," AIAA Paper 72–174, San Diego, Calif., 1972.

[6] Argyris, J. H., and Dunne, P. C., *Structural Principles and Data*, edited by D. M. A. Leggett and M. Langley, Pitman Press, London, 1934.

[7] Yoshika, Y. and Kawai, T., "On the Method of Application of Energy Principles to Problems of Elastic Plates," *Applied Mechanics, Proceedings of the 11th International Congress of Applied Mechanics, Munich (Germany) 1964*, edited by H. Gortler, Springer-Verlag, Berlin, 1966.

[8] Kruszewski, E. T., Kordes, E. E., and Weidman, D. J., "Theoretical and Experimental Investigations of Delta-Wing Vibrations," TN 4015, June 1957, NACA.

[9] Levy, S., "Structural Analysis and Influence Coefficients for Delta-Wings," *Journal of the Aeronautical Sciences*, Vol. 20, No. 7, July 1953, pp. 449–454.